Supplemental Material for

Impact of Ga and N vacancies at the GaN *m*-plane on the carrier dynamics of micro-light-emitting diodes

Purun-hanul Kim,[1] Sang Ho Jeon,[2] Jin Hyuk Jang,[2] Seungwu Han,[1] and Youngho Kang [3,*]

[1] *Department of Materials Science and Engineering and Research Institute of Advanced Materials, Seoul National University, Seoul 08826, Korea*

[2] *Display Research Center, Samsung Display Co. Ltd., Yongin-si, Gyeonggi-do 17113, Korea*

[3] *Department of Materials Science and Engineering, Incheon National University, Seoul 08826, Korea*

S1. A detailed explanation of the 2D Freysoldt correction scheme

Δ^q in equation 1 in the main text is a finite size correction term that is important for correcting electrostatic artifacts caused by charged defects within periodic boundary conditions. For repeated slab (2D) and bulk (3D) calculations, Freysoldt et al. suggested surrogate electrostatic models that can calculate Δ^q [1, 2]. In these schemes, Δ^q comprises a periodicity correction of a charged system and a potential alignment-like term. The first term is calculated from the electrostatic interaction energy between repeated Gaussian model charges in a dielectric medium. In this case, the homogeneous background of a compensating charge (called jellium) is considered. The alignment-like term occurs due to the misalignment of the potentials between the DFT and model calculations. This term in slab calculations can be obtained by making the short-range potential in the vacuum region flat and zero, as shown in Fig. S4. In this figure, V_{model} is a model potential, ΔV_{DFT} is a defect-induced change in the DFT electrostatic potential, and V_{sr} is a short-range potential that corresponds to the difference between V_{model} and ΔV_{DFT}

S2. Test of the 2D Freysoldt scheme with respect to slab thickness and vacuum.

To check if the 2D Freysoldt model well works, we calculated the vacancy formation energy for V_N in the 1+ charge state on the *m* plane with respect to the vacuum height up to 25 Å, as shown in Fig. S1a. Without the correction, the formation energy grows with an increase of the vacuum height, whereas the value remains constant when applying the correction. In addition, in Fig. S1b, we calculated the formation energy going away from the surface to the bulk region considering the 2D Freysoldt correction. We found that the formation energy approaches the one obtained in the bulk calculation. These results confirm that the correction scheme is reliable.

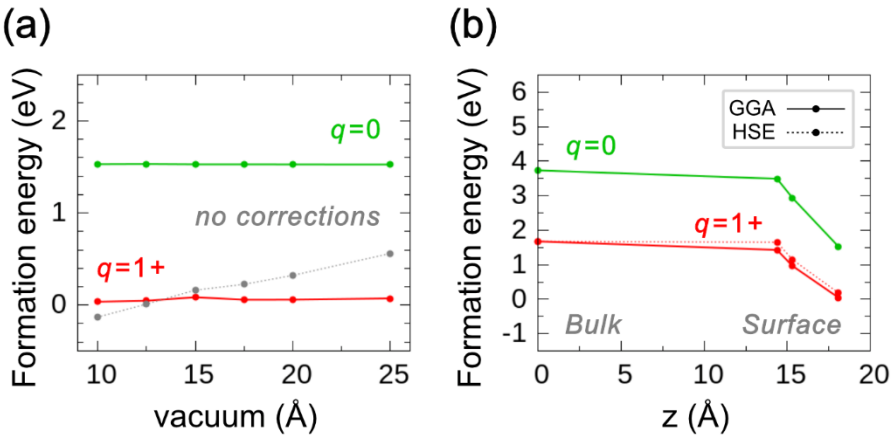

FIG. S1. V_N formation energies with the Freysoldt correction scheme in structures with (a) different vacuum heights and (b) defect positions. The formation energies were calculated using the PBE functional in (a) and (b) and a hybrid functional in (b) as well.

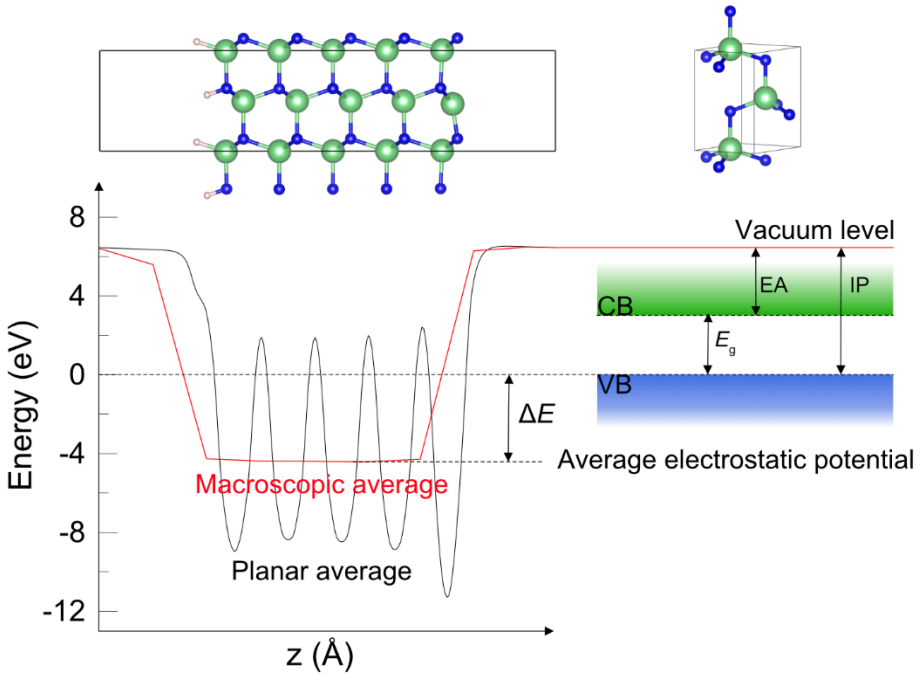

FIG. S2. Schematics of obtaining the valence band maximum (VBM) of the GaN surface model from the bulk band structure by aligning the electrostatic potential. The black solid line is the planar averaged Coulomb potential. The red solid line is the macroscopically averaged Coulomb potential. ΔE corresponds to the VBM position with respect to the macroscopic average of the Coulomb potential of the slab model.

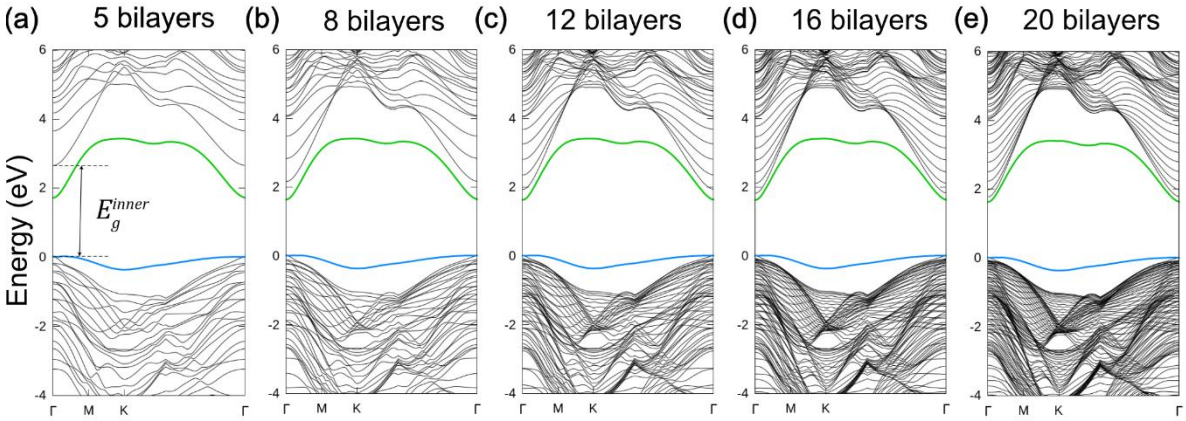

FIG. S3. (a-e) Band structures of 5 to 20 bilayer slab models calculated with the PBE functional. The blue and green lines are related to the N and Ga dangling bonds, respectively. With an increase in the number of bilayers, the conduction (valence) band edge approaches the Ga(N) dangling bond states at Γ, reducing the bandgap of the bulk part in the slab models (E_g^{inner}).

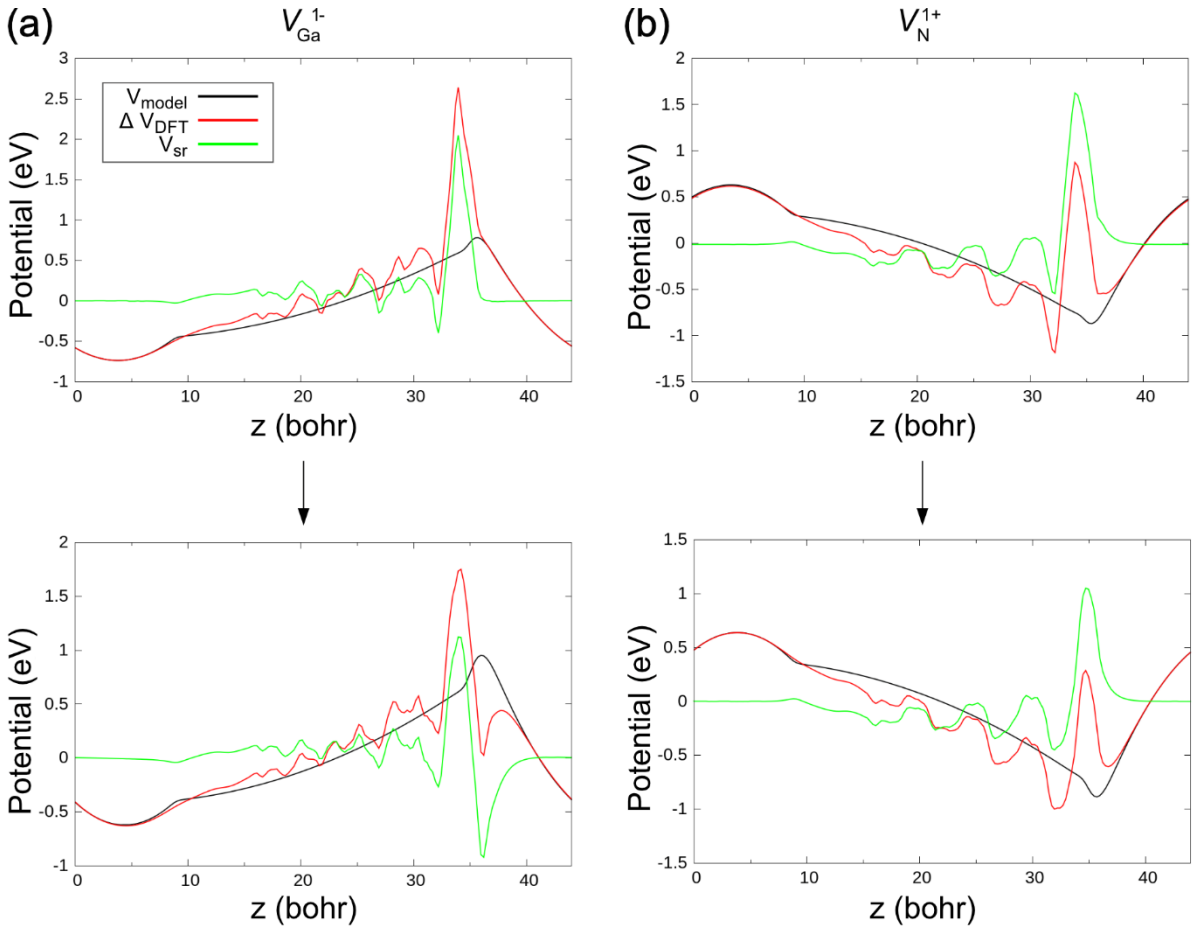

FIG. S4. Potential profiles of (a) V_{Ga}^{1-} and (b) V_{N}^{1+} on the *m* plane before (upper figures) and after (lower figures) potential alignment to calculate the correction term for the defect formation energy by the 2D Freysoldt correction scheme. Black line ($\mathrm{V_{model}}$): potential from the surrogate model; red line ($\Delta\mathrm{V_{DFT}}$): defect-induced change in the DFT electrostatic potential; and green line ($\mathrm{V_{sr}}$): short range potential.

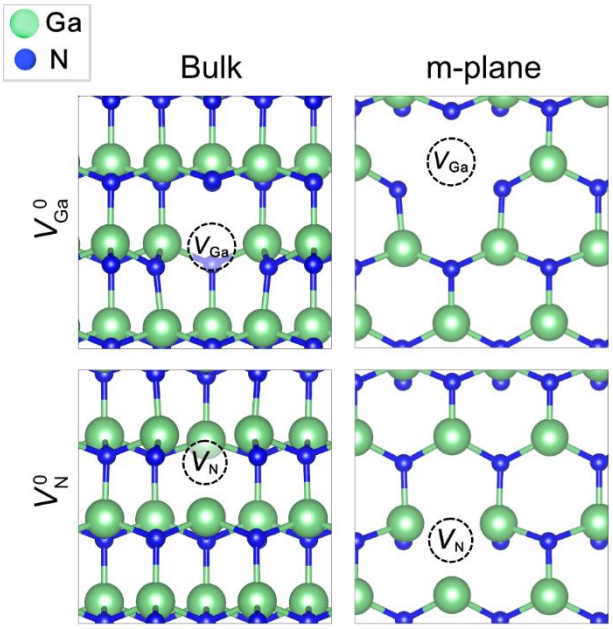

FIG. S5. Atomic structures of V_{N}^{0} and V_{N}^{1+} on the *m* plane and in the bulk.

S3. Charge distributions of a surface and bulk nitrogen vacancy.

Fig. S6 (a) and (b) illustrate the charge distributions of the one of the defect states associated with $V^0_{\mathrm{N,surf}}$ and $V^0_{\mathrm{N,bulk}}$, respectively. The defect states of $V^0_{\mathrm{N,surf}}$ and $V^0_{\mathrm{N,bulk}}$ mainly derive from the hybridization of three and four neighboring Ga dangling bonds, respectively, and several electronic states with different energies are formed for each defect depending on the hybridization manner (i.e., bonding or antibonding manners). In $V^+_{\mathrm{N,surf}}$ and $V^+_{\mathrm{N,bulk}}$, the charge distributions slightly change compared to those of corresponding neutral states. However, the major constituting orbitals and the bonding characteristics are still maintained.

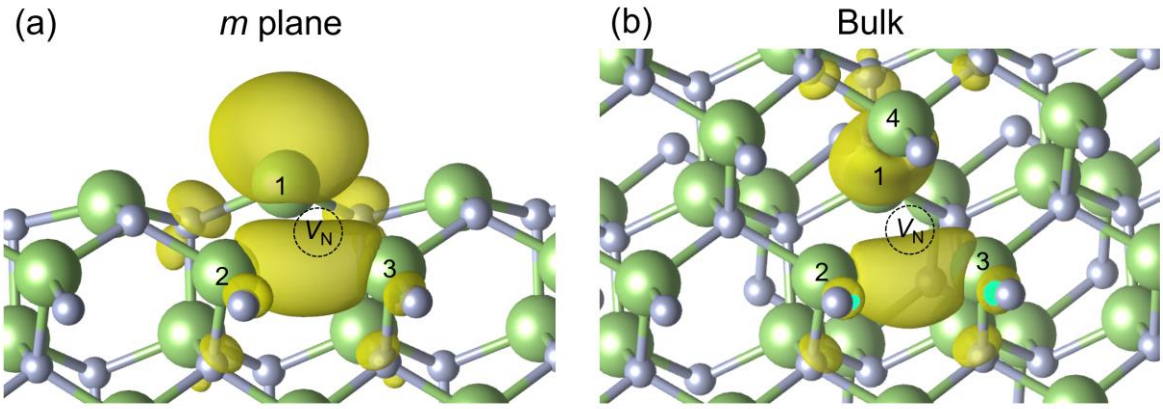

FIG. S6. Charge density distributions of (a) $\boldsymbol{V^0_{\mathrm{N,surf}}}$ (isovalue = 0.0040 e/Å^3) and (b) $\boldsymbol{V^0_{\mathrm{N,bulk}}}$ (isovalue = 0.0064 e/Å^3). Green and blue balls indicate Ga and N atoms, respectively.

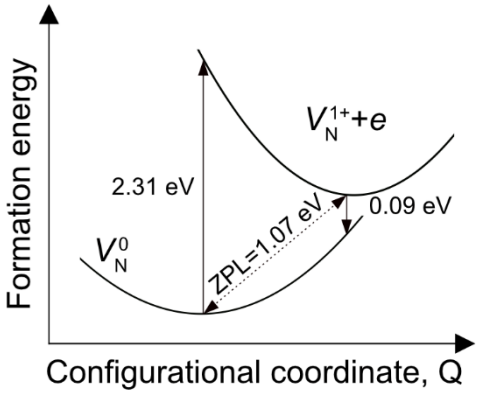

FIG. S7. Schematic configurational coordination diagram for V_{N} illustrating the optical transition of $V_{\mathrm{N,surf}}^{0} \rightarrow V_{\mathrm{N,surf}}^{1+} + e^{-}$.

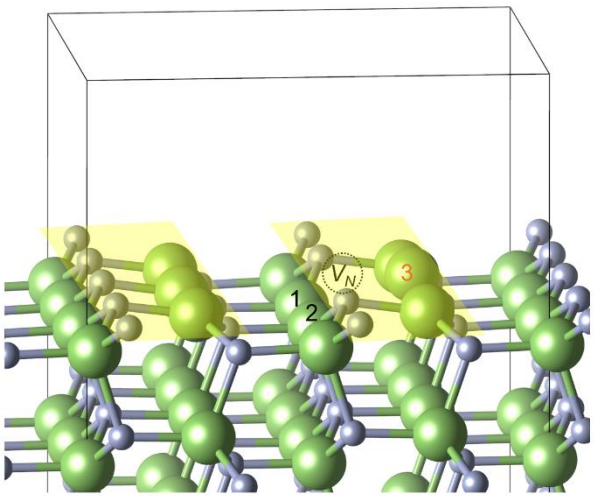

FIG. S8. Atomic structure of the *m* surface with $\boldsymbol{V}_{\mathbf{N}}$ at the top surface. '1' and '2' represent subsurface Ga atoms, and '3' represents a top-surface Ga atom. The atoms in the yellow plane correspond to top-surface atoms in the slab model. Green and blue balls indicate Ga and N, respectively.

Table S1. Effective parameters for V_N related to luminescence transitions in GaN. ΔQ: total mass-weighted distortions; Ω^2: square effective vibration; $\hbar\Omega$: energies of effective vibrations; and S: Huang-Rhys factors [3].

V_N	ΔQ [amu$^{1/2}$Å]	Ω^2 [eV/(amu$^{1/2}$Å)^2]	$\hbar\Omega$ [meV]	S (Huang-Rhys factor)
Bulk (q = +1)	2.791	0.084	18.723	17.443
Bulk (neutral)	2.791	0.089	19.280	17.961
m-plane (q = +1)	4.449	0.059	15.651	37.042
m-plane (neutral)	4.449	0.050	14.445	34.189

References

[1] C. Freysoldt and J. Neugebauer, First-Principles Calculations for Charged Defects at Surfaces, Interfaces, and Two-Dimensional Materials in the Presence of Electric Fields, Phys. Rev. B Condens. Matter **97**, 205425 (2018).

[2] C. Freysoldt, J. Neugebauer, and C. G. Van de Walle, Fully ab initio finite-size corrections for charged-defect supercell calculations, Phys. Rev. Lett. **102**, 016402 (2009).

[3] A. Alkauskas, Q. Yan, and C. G. Van de Walle, First-Principles Theory of Nonradiative Carrier Capture via Multiphonon Emission, Physical Review B. **90**, 075202 (2014).